ZESZYTY NAUKOWE AKADEMII MARYNARKI WOJENNEJ
SCIENTIFIC JOURNAL OF POLISH NAVAL ACADEMY

2016 (LVII) 1 (204)

DOI: 10.5604/0860889X.1202434

Daniel Gapiński*

ANALYSIS OF IMPACT OF DISRUPTIONS COMING FROM A SHIP ON THE ACCURACY OF DETERMINING THE LOCATION OF THE TRACKED AIR TARGET BY THE MODIFIED OPTOELECTRONIC SCANNING AND TRACKING IR SEEKER

ABSTRACT

The paper presents the results of research whose aim was to specify the impact of disruptions coming from the movement of a ship on the accuracy of determining the location of the tracked target by the modified, optoelectronic scanning and tracking seeker (OSTS). The basic task of OSTS consists in detecting and then tracking closely the detected air target, emitting infrared radiation.

Key words:
self-guided seeker, detecting, tracking, disruptions, IR seeker.

INTRODUCTION

The process of detecting air attack means (AAM) in air space on small distances (up to 6 km) may be done directly by operators (anti-aircraft gunners) equipped e.g. with optical day or night-vision sights. However, due to the constant development of AAM, the visual detection and determination of flight parameters of a target is becoming less and less effective, and more and more frequently on short

* Kielce University of Technology, Faculty of Mechatronics and Mechanical Engineering, 1000-lecia PP 7 Str., 25-314 Kielce, Poland; e-mail: dgapinski@tu.kielce.pl

distances it is replaced by advanced systems of automatic detection and tracking. Automatic searching in space can be done with an active, semi-active or passive method. The first two methods consist in sending most often electromagnetic waves into the air space from the observation position and then receiving the radiation reflected from the target (the so called echo). The drawback of the above methods is that the tracked object may detect that it is being tracked and in this way learn the location of observation positions from which it was radiated. Whereas, the passive method consists in detecting own radiation that is emitted by the target itself (usually electromagnetic infrared waves) thanks to which the target is not able to detect that it is being tracked. After locating the target, the detecting system should determine its location, and then commence the tracking in order to guide, e.g. an anti-aircraft rocket missile. The designed, passive scanning and tracking IR seeker [8] allows to aim a missile only in the direction of the predicted appearance of the target. The optical axis of the seeker does program movements [5, 10] and simultaneously the system of mirrors scans the air space with the so called big scanning angle. It increases the area of searching and, with the suitable selection of speed of the programmed movement, gives satisfactorily dense scanning of space. At the moment of intercepting the target by the seeker, angles by which its axis is to be moved so that it overlapped with the target observation line (LOC) are determined. It is still the program control which can be carried out, e.g. in a straight line with the so called overtaking angle [7, 9]. After intercepting the target and the programmed resetting of the seeker axis on LOC, there is the second phase consisting in tracking it. During that phase, the seeker passes into the second mode of operation in which the set angles of scanning mirrors [11] are decreased as a result of which the scanned area of space is narrowed down, while the control of the seeker axis is performed based on the angular coordinates of the target which are determined on an ongoing basis by the optoelectronic system of the device. During the programmed search of the air space by OSTS and while tracking the already detected target, there may appear negative forces coming from the movements of the missile launcher in which a missile is placed. Those movements may be caused directly by the gunner holding the missile launcher on their shoulder unsteadily, or by the movement of the ground on which the launcher is placed, e.g. the deck of the ship at sea. In light of the above, it is necessary to conduct the analysis of impact of the above disruptions on the accuracy of control of the OSTS axis as well as on the accuracy of determining angular coordinates of the detected target.

MATHEMATICAL MODEL

To perform the analysis whose aim is to examine the impact of the disruptions coming from the movement of a ship floating on waves on the process of detecting and tracking an air target by OSTS, the model of the above phenomenon was adopted according to [29] categorizing the movements of the ship in accordance with six degrees of freedom. Figure 1a shows main components of oscillatory movement of a ship on the surface of sea, while figure 1b shows the double anti-aircraft short-range rocket missile launcher that is mounted on the ship. Figure 1c shows the diagram of the designed IR seeker, including the adopted systems of coordinates as well as markings of individual angles of rotation of respective systems in relation to one another. When considering the movements of a ship floating on the surface of sea, the beginning of the system of coordinates $x\,y\,z$ was adopted that is connected with the ship in its centre of gravity G. Due to the analysed problem connected with detecting and tracking air targets, axis z of the above system was directed upwards, axis x was directed towards the bow, while axis y towards the left side. The movements of the ship floating on waves, marked in figure 1a, are defined as follows: 1 — heave, 2 — sway, 3 — surge, 4 — pitch, 5 — yaw, 6 — roll. The angle of lateral tilt of the ship caused by rolling is marked as τ_x, the angle of longitudinal tilt of the ship caused by pitching is marked as τ_z, while swamping a ship which is the result of yawing is marked as τ_y. It was assumed that the launcher mounted on the ship may perform additional angular movements in the horizontal plane (azimuth) marked with number 7 in figure 1b and with number 8 in the vertical plane. The marking of launcher rotation angle was adopted in azimuth as ψ_W and in altitude as γ_W.

The law of scanning the air space by the optoelectronic system of OSTS was presented in [3] and we will write it in the following way:

$$\beta_x(t) = a\tan(\tan(\beta(t)) \cdot \cos(a\sin(z_{zp}(t)/\sqrt{x_{zp}(t)^2 + z_{zp}(t)^2})) \tag{1}$$

$$\beta_z(t) = a\tan(\tan(\beta(t)) \cdot \sin(a\sin(z_{zp}(t)/\sqrt{x_{zp}(t)^2 + z_{zp}(t)^2})) \tag{2}$$

where:

$\beta_X(t)$, $\beta_Z(t)$ — angular coordinates of the detected target in relation to the scanning seeker axis;

$\beta(t)$ — the resultant angle of deflection of a light beam from the optical axis;

x_{zp} , z_{zp} — components of the location of a light beam on the surface of the primary mirror.

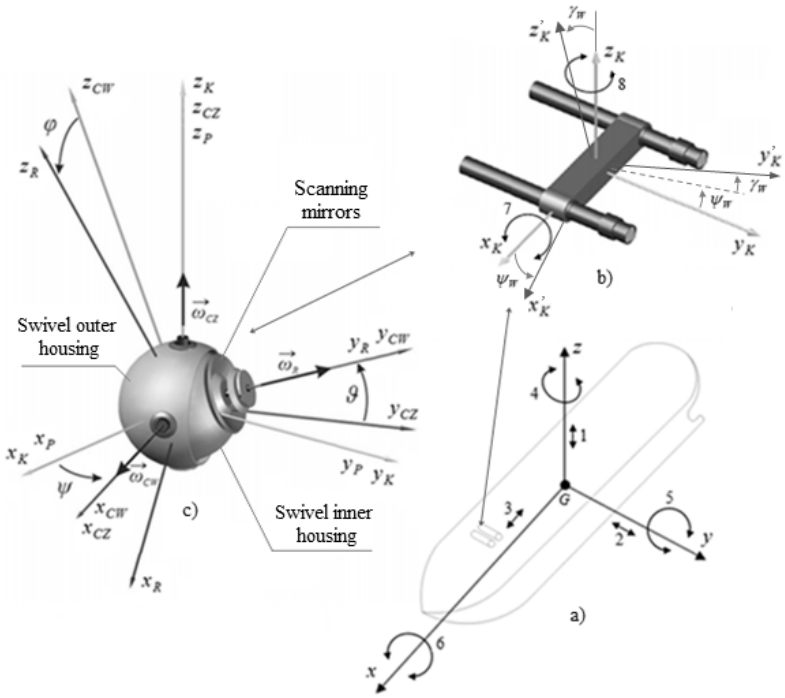

Fig. 1. The adopted systems of coordinates

The resultant angular movements of missile body in which the seeker is mounted are treated as external disruptions and have been determined with the use of angular speeds: $\omega_{x_P}, \omega_{y_P}, \omega_{z_P}$, causing the rotation of the body around individual axes of the system $x_P\ y_P\ z_P$ by appropriate angles $\alpha_x\ \alpha_y\ \alpha_z$.

The following systems of coordinates were introduced:

$x\ y\ z$ — the system of coordinates connected with the ship;

$x_K\ y_K\ z_K$ — the system of coordinates connected with the missile launcher, determining the reference direction for OSTS in space;

$x_R\ y_R\ z_R$ — the moving system of coordinates connected with the rotor of the IR seeker;

$x_{CW}\ y_{CW}\ z_{CW}$ — the moving system of coordinates connected with the inner housing;

$x_{CZ}\ y_{CZ}\ z_{CZ}$ — the moving system of coordinates connected with the outer housing;

$x_P\ y_P\ z_P$ — he moving system of coordinates connected with the missile.

The following markings of individual angles of rotation were adopted:

τ_x — the angle of lateral tilt of a ship caused by rolling;

τ_y — the angle of swamping a ship which is the result of yawing;

τ_z — the angle of longitudinal tilt of a ship caused by pitching;

ψ_W, γ_W — the angles of rotation of the rocket missile launcher in azimuth and in altitude respectively;

ψ — angle of rotation $x_{CZ}\ y_{CZ}\ z_{CZ}$ in relation to $x_K\ y_K\ z_K$ around axis z_{CZ};

ϑ — angle of rotation $x_{CW}\ y_{CW}\ z_{CW}$ in relation to $x_K\ y_K\ z_K$ around axis x_{CW};

φ — angle of rotation $x_R\ y_R\ z_R$ in relation to $x_K\ y_K\ z_K$ around axis y_R;

α_x — angle of rotation $x_P\ y_P\ z_P$ in relation to $x_K\ y_K\ z_K$ around axis x_P;

α_y — angle of rotation $x_P\ y_P\ z_P$ in relation to $x_K\ y_K\ z_K$ around axis y_P;

α_z — angle of rotation $x_P\ y_P\ z_P$ in relation to $x_K\ y_K\ z_K$ around axis z_P.

Hence, the location of the IR seeker axis in relation to the system $x_K\ y_K\ z_K$ is determined with the use of three angles: ψ, ϑ, φ. Angles ψ, ϑ are measured with the use of fibre-optic sensors, while angle φ is measured with rotor location sensor [8].

As given quantities the following were adopted:

1. $J_{x_{CZ}}, J_{y_{CZ}}, J_{z_{CZ}}$ — calculated moments of complete inertia of the outer housing.
2. $J_{x_{CW}}, J_{y_{CW}}, J_{z_{CW}}$ — calculated moments of complete inertia of the inner housing.
3. $J_{x_R}, J_{y_R}, J_{z_R}$ — calculated moments of inertia of the rotor.
4. $\vec{\omega}_P\left(\omega_{x_P}, \omega_{y_P}, \omega_{z_P}\right)$ — angular speed of the missile body.
5. $\vec{M}_Z$ — moment of missile forces having an impact on the outer housing.
6. $\vec{M}_W$ — moment of missile forces having an impact on the inner housing.
7. $\vec{M}_{TW}, \vec{M}_{TZ}$ — moments of friction forces in bearings in inner and outer housing respectively, however $\vec{M}_{TW} = c_w\dot{\vartheta}$, $\vec{M}_{TZ} = c_z\dot{\psi}$, where c_w, c_z are friction coefficients in bearings of the inner and outer housing respectively.

Based on the adopted physical model of OSTS, using Lagrange II-nd kind of equations, the equations of the seeker movement were derived [4, 16–19, 21]:

$$\begin{aligned} M_Z = {} & M_{TZ} + J_{z_{CZ}} \frac{d}{dt}\omega_{z_{CZ}} + J_{y_{CW}} \frac{d}{dt}\left(\omega_{y_{CW}} \sin\vartheta\right) + \\ & + J_{z_{CW}} \frac{d}{dt}\left(\omega_{z_{CW}} \cos\vartheta\right) + J_{y_R} \frac{d}{dt}\left(\omega_{y_R} \sin\vartheta\right) + \\ & + J_{z_R} \frac{d}{dt}\left(\omega_{z_R} \cos\vartheta\right) - \left(J_{x_{CZ}} - J_{y_{CZ}}\right)\omega_{x_{CZ}}\omega_{y_{CZ}} + \\ & - \left(J_{x_{CW}} + J_{x_R}\right)\omega_{x_{CW}}\omega_{y_{CZ}} + J_{y_{CW}}\omega_{y_{CW}}\omega_{x_{CZ}}\cos\vartheta + \\ & - \left(J_{z_{CW}} + J_{z_R}\right)\omega_{z_{CW}}\omega_{x_{CZ}}\sin\vartheta + J_{y_R}\omega_{y_R}\omega_{x_{CZ}}\cos\vartheta \end{aligned} \tag{3}$$

$$\begin{aligned} M_W = {} & M_{TW} + J_{x_{CW}} \frac{d}{dt}\omega_{x_{CW}} + J_{x_R} \frac{d}{dt}\omega_{x_{CW}} + \\ & - \left(J_{y_{CW}} - J_{z_{CW}} - J_{z_R}\right)\omega_{y_{CW}}\omega_{z_{CW}} - J_{y_R}\omega_{y_R}\omega_{z_{CW}} \end{aligned} \tag{4}$$

where:

angular speed of the rotor of the seeker

$\omega_{y_R} = n$;

angular speeds of the outer housing

$\omega_{x_{CZ}} = \omega_{x_P}\cos\psi + \omega_{y_P}\sin\psi$, $\omega_{y_{CZ}} = -\omega_{x_P}\sin\psi + \omega_{y_P}\cos\psi$, $\omega_{z_{CZ}} = \dot{\psi} + \omega_{z_P}$;

angular speeds of the inner housing

$\omega_{x_{CW}} = \omega_{x_{CZ}} + \dot{\vartheta}$, $\omega_{y_{CW}} = \omega_{y_{CZ}}\cos\vartheta + \omega_{z_{CZ}}\sin\vartheta$, $\omega_{z_{CW}} = -\omega_{y_{CZ}}\sin\vartheta + \omega_{z_{CZ}}\cos\vartheta$.

Parameters of OSTS

Moments of inertia of the rotor relative to the axis x_R, y_R, z_R:

$J_{x_R} = 0{,}00158446\ \mathrm{kg\cdot m^2}$, $J_{y_R} = 0{,}0011405\ \mathrm{kg\cdot m^2}$, $J_{z_R} = 0{,}00158124\ \mathrm{kg\cdot m^2}$.

Moments of inertia of the complete inner housing relative to the axis x_{CW}, y_{CW}, z_{CW}:

$J_{x_{CW}} = 0.0004453\ \mathrm{kg\cdot m^2}$, $J_{y_{CW}} = 0{,}0006437\ \mathrm{kg\cdot m^2}$, $J_{z_{CW}} = 0{,}0004721\ \mathrm{kg\cdot m^2}$.

Moments of inertia of the complete outer housing relative to the axis x_{CZ}, y_{CZ}, z_{CZ}:

$J_{x_{CW}} = 0{,}00020254\ \mathrm{kg\cdot m^2}$, $J_{y_{CW}} = 0{,}0003237\ \mathrm{kg\cdot m^2}$, $J_{z_{CW}} = 0{,}000249\ \mathrm{kg\cdot m^2}$.

Friction coefficient in the bearing of inner housing: $c_w = 0{,}05\ \mathrm{N \cdot m \cdot s}$.

Friction coefficient in the bearing of outer housing: $c_z = 0{,}05\ \mathrm{N \cdot m \cdot s}$.

Rotary velocity of the rotor: $n = 1050\ \mathrm{rad/s} \approx 10000\ \mathrm{obr/min}$.

Weight of complete seeker: $m_G = 2{,}25\ \mathrm{kg}$.

Maximum torque of the motors for control the individual seeker housings: $M_{\max} = 1{,}5\ \mathrm{N \cdot m}$.

Parameters of ship movement on sea waves

The movements of a ship floating on waves are a complex phenomenon, caused among others by free oscillation of sea surface, wind, the buoyancy of a sailing unit, its speed, or the direction of wave [20, 29]. The periods of free tilt of the body also depend on whether vessel centre of mass exceeds its buoyancy and on the dimensions of the body itself. These periods decrease along with the buoyancy of the ship, while also the length and height of sea wave has an impact on the values of tilt angles. That is why it is important to determine both the parameters of the ship on which the rocket missile launcher is mounted, as well as the condition of sea during which fire actions are to be conducted. Due to the critical parameters of forces which have an impact on the reliable operation of OSTS [6], it was assumed that the IR seeker operates on a small unit with small buoyancy of 200 t (e.g. minesweeper type 207 M) [23, 24] and the completion of combat tasks is performed with the condition of sea up to 4 on the Beaufort scale. For the above assumptions, maximum tilt amplitudes of the body have been determined at the level of $A = 26^o$ and the frequency of their occurrence in scopes of $f = 0{,}5 - 0{,}125\ \mathrm{Hz}$. The presented above, oscillation movements of a ship floating on waves are variable in time. The movements themselves of the free surface of sea are unstable phenomena, occurring in an irregular way and at random. Adopting a regular model of the ship tilt (e.g. through the sinusoidal function) for the above conditions does not make sense. Irregular models of ships oscillations are prepared mainly with the use of characteristics of distribution of random variables considering the dependences between longitudinal and side tilt values, their speeds and accelerations in the considered period of time [2, 13, 15, 28]. The resultant disruption in any point of the area, which is reached by various waves of the same kind, is the algebraic total of disruptions caused in that point by each wave separately, what is the basic premise of the so called superposition of waves [27]. Other ways of modelling ship movements on waves may be their direct measurement on the deck of the sailing unit or laboratory observation of miniature ships on observation positions [1, 22, 25, 26].

In the above paper will be presented different from those mentioned above a way of modelling dynamic oscillations of a ship on waves. This oscillations will then be used as the disruptive phenomena for the examined OSTS. According to the above conducted analysis, maximum amplitudes have been determined as well as the ranges of their frequency for oscillations of a given type of ship with the assumed condition of sea. With view to the fact that detecting and tracking an air target by OSTS is a relatively short process and considering the random nature of oscillations of a ship on waves, such type of sample phenomena can easily be drawn, what was presented in figure 2. To be sure as to the continuity of the drawn line and of the fact that the 'process does not go back in time', i.e. that the direction of the drawn line always runs from left to right, one should use the software that enables precise drawing based on the system of coordinates and saving vector files, e.g. AutoCAD software.

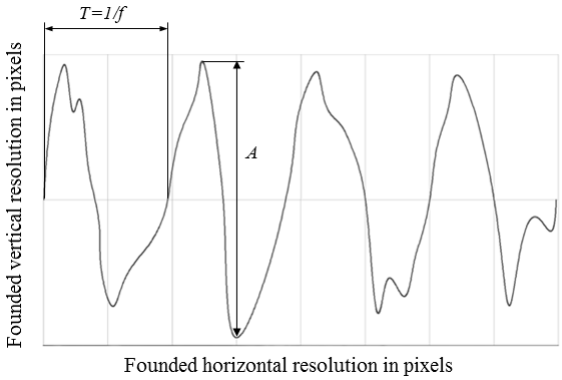

Fig. 2. An example of the oscillations ship drawn in AutoCAD

The drawn graph (fig. 2) is saved in the planned resolution in a file that enables its further graphical processing. The time of phenomenon occurrence is reflected on the horizontal axis, while its values on the vertical axis. For example, if the total time of graph shown in figure 2 is to amount to $t = 8\,\mathrm{s}$, while the maximum amplitude $A = 20^{o}$ and the file was saved in the resolution of 1366x768, then the sampling sequence of the time axis will amount to $\Delta t = \frac{\mathrm{t}}{1366} = 0{,}005857$ and for the axis of function values to $\Delta A = \frac{A}{768} = 0{,}026042$.

If the obtained sampling parameters are not satisfactory, then fragments of the file may be increased by vectors, and thus its resolution may be increased, or the data obtained from the file may be subjected to polishing up and further numerical processing. The next step is differentiation after the time of the data obtained from

the file and thereby calculating the speed and accelerations of the occurrence of the phenomenon. For polishing up data the averaging algorithm was used, while for the numerical decrease of the sampling sequence the algorithms similar to the ones used in paper [12] were used or similar to the method of Simpson's approximated integration [14] with the difference that the divided period between consecutive sampling sequences is not replaced with a vector function or a second degree polynomial, but the averaging function. Decreasing the sampling sequence is done in accordance with the pre-calculated accelerations, and then the process is reversed, i.e. speed and movement of the simulated phenomenon are determined using integration. All operations have been performed based on own software written in C++ language. Figures 3–6 show the results of numerical processing of a file with the buoyancy shown in figure 2 which can be treated as the dynamic rolling of a ship on sea waves. Figure 3 shows the calculated angular speeds of a ship $\ddot{\tau}_x$, while figure 4 shows angular speeds of the above phenomenon $\dot{\tau}_x$. Figure 5 shows the calculated course of rolling of a ship after poliship up data and the numerical decrease of the sampling sequence what was shown in figure 6.

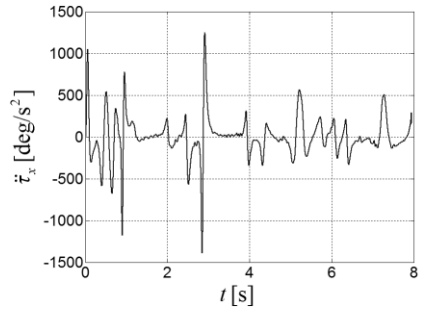

Fig. 3. Simulation of the angular acceleration roll motion resulting from the digital processing the graph shown in fig. 2

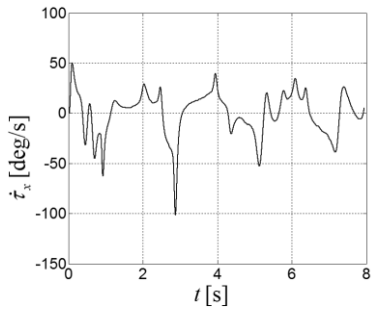

Fig. 4. Calculated angular velocity roll motion for acceleration shown in fig. 3

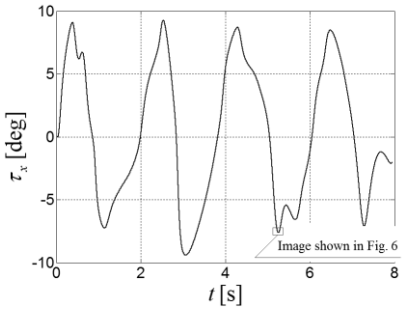

Fig. 5. Calculated values roll motion for acceleration shown in fig. 3

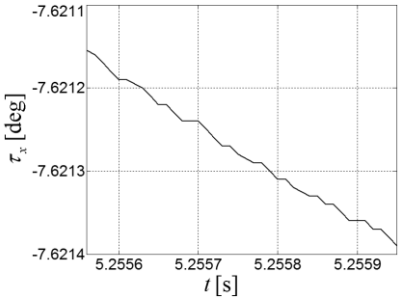

Fig. 6. An enlarged section of fig. 5 showing a numerical reduction in the sampling step

Parameters of launcher movement

Apart from the forces coming from oscillations of the ship floating on sea waves disrupting the operation of OSTS, also additional forces in the form of movements of the rocket missile launcher itself independent of ship movements should be taken into consideration. Two types of that sort of disruptions were considered in the paper. The first pertains to the launcher mounted directly on the ship (fig. 1a, b) where the launcher may perform additional angular movements in azimuth and in altitude. Due to limitations resulting from permissible angular speeds for individual OSTS housings [20] which maximally amount to 70°/s (in the case of seeker operation without external disruptions), it should be adopted initially that maximum angular speeds of launcher movements in its programmed resetting on the detected target cannot exceed the above value. The second considered case of disruptions are random movements of a single launcher, held on a shoulder by a gunner who is on the deck of a ship.

RESEARCH RESULTS AND CONCLUSIONS

Below are presented selected examples of computer simulation of the analysis of impact of disruptions coming from a sea ship as well as the movements of the launcher mounted on its deck, on the accuracy of controlling the OSTS axis as well as on the accuracy of determining angular coordinates of the detected air target.

Verifying the operation of OSTS in the mode of searching the air space on the surface of a circular cone with the simultaneous consideration of forces coming from the movements of the launcher located on the shoulder of a gunner

Apart figures 7–12 shows the forces coming from a sudden movement of the rocket missile launcher which was caused by the gunner holding it on his shoulder. Accelerations of the launcher and thereby the axis of a rocket missile which is located in it are shown in figures 9–10. Figure 13 shows the trajectories of programmed movement of the seeker axis and the trajectory of movement of rocket missile axis, caused by forces coming from the rocket missile launcher. Figures 11 and 12 show the moments controlling individual OSTS housings, with the consideration of the impact of disruptive forces and without, respectively.

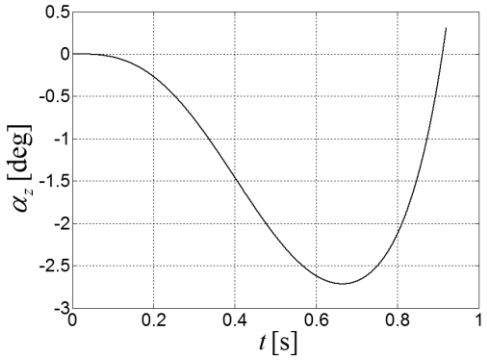

Fig. 7. Rotation of the missile around the z_P axis of the projectile caused by the movement of the launcher located on the shoulder of the shooter

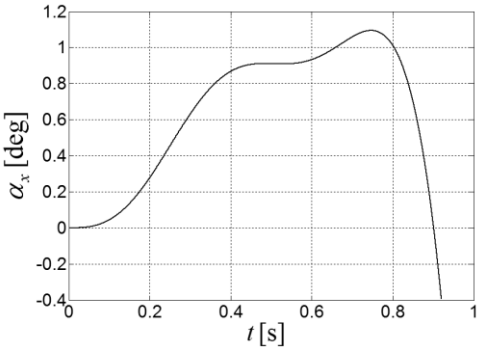

Fig. 8. Rotation of the missile around the z_P axis of the projectile caused by the movement of the launcher located on the shoulder of the shooter

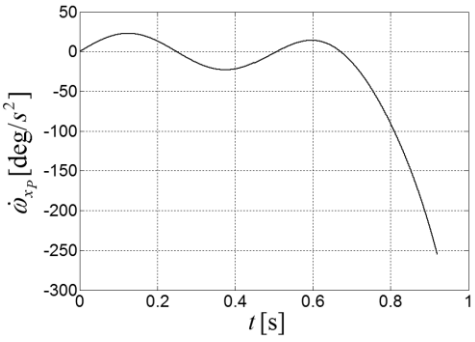

Fig. 9. The angular acceleration of extortion which is shown in fig. 7

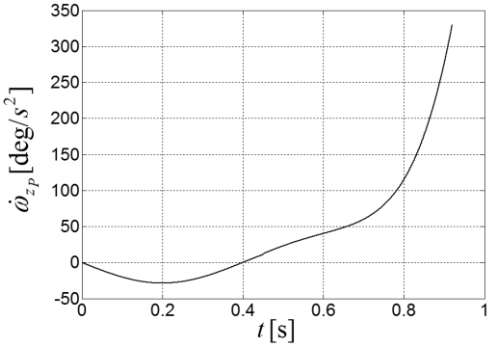

Fig. 10. The angular acceleration of extortion which is shown in fig. 8

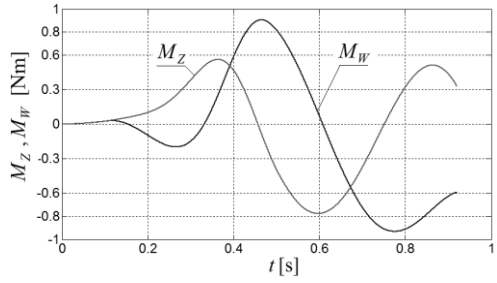

Fig. 11. Control moments of the IR scanning seeker taking into account oscillations disturbing coming from ship

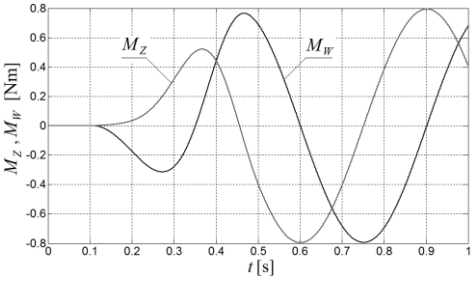

Fig. 12. Control moments of the outer M_Z and inner housing M_W (IR scanning seeker) no taking into account oscillations disturbing coming from ship

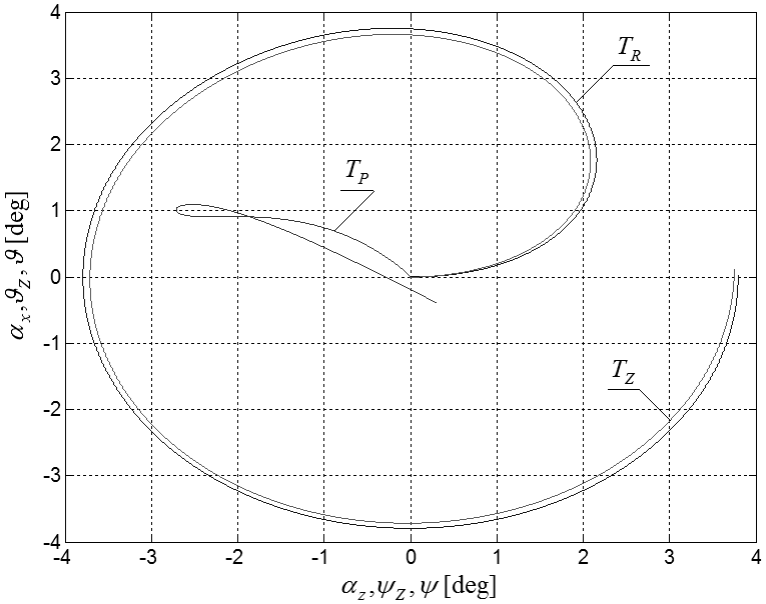

Fig. 13. Trajectory of the set TZ and actual TR movement of the seeker axis and trajectory movement of the missile axis

It appears from the diagrams of trajectories of movement set and performed by the OSTS axis shown in figure 13 that the forces shown above do not have a significant impact on the process of controlling the seeker, while when compared to figures 11 and 12 it appears that they cause the increase of controlling moments in a permissible scope.

Verifying the operation of OSTS in the mode of searching the air space on the surface of an unwinding spiral with the consideration of forces coming from a sea ship with the condition of sea of 3 B

Figures 14–19 shows the forces coming from the movements of the ship on waves having an impact on the missile launcher mounted on its deck (fig. 1a, 1b) and thereby on OSTS. Accelerations and angular speeds of the launcher are shown in figures 17–19 respectively. Figure 22 shows the trajectories of programmed movement of the seeker axis and the trajectory of movement of rocket missile axis, caused by oscillations of a ship.

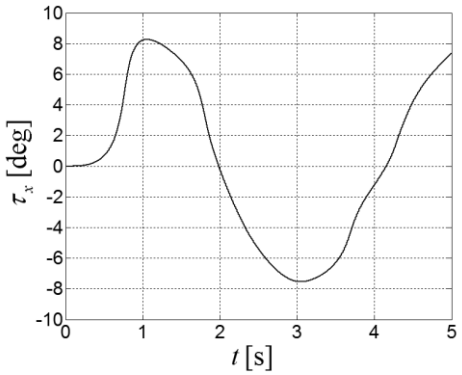

Fig. 14. Roll motion of the ship

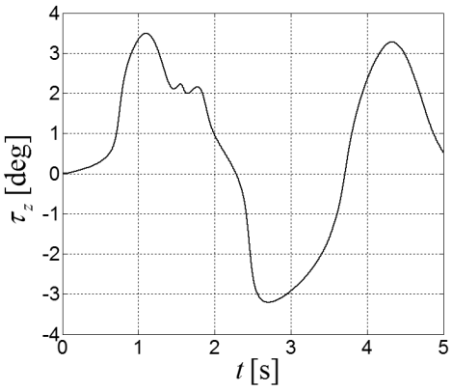

Fig. 15. Yaw motion of the ship

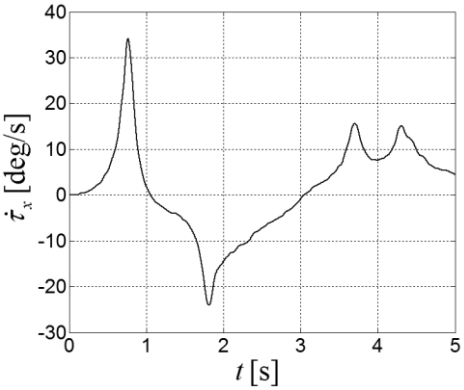

Fig. 16. Angular velocity roll motion

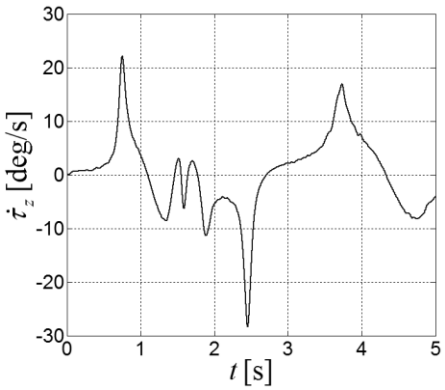

Fig. 17. Angular velocity yaw motion

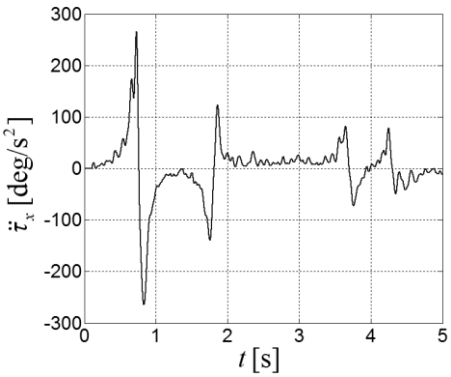

Fig. 18. Angular acceleration roll motion

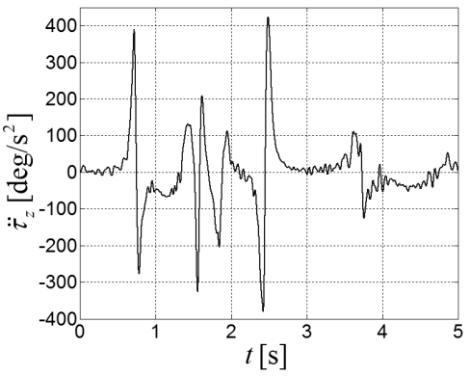

Fig. 19. Angular acceleration yaw motion

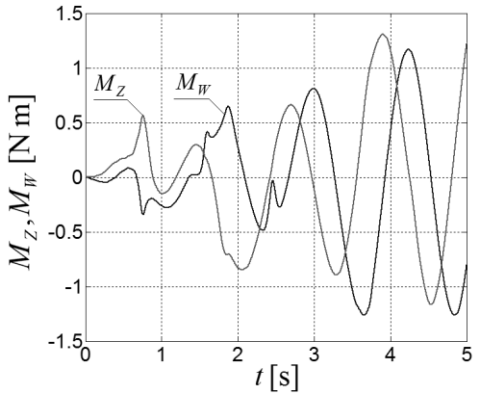

Fig. 20. Control moments of the scanning seeker taking into account oscillations disturbing coming from ship

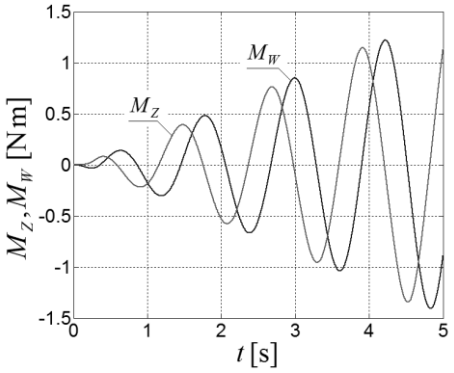

Fig. 21. Control moments of the scanning seeker no taking into account oscillations disturbing coming from ship

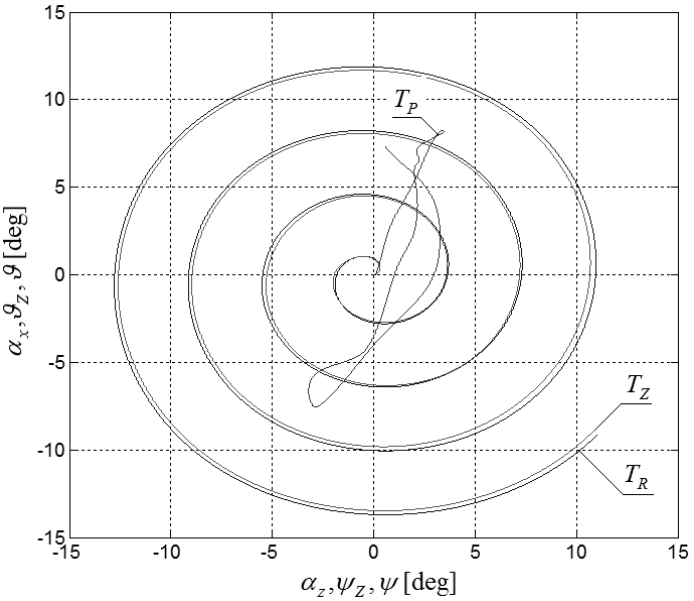

Fig. 22. Trajectory of the set T_Z and actual T_R movement of the seeker axis and trajectory movement of the missile axis T_P

It appears from the diagrams of trajectories of movement set and performed by the OSTS axis shown in figure 22 that the forces shown above do not have a significant impact on the process of controlling the seeker, while when compared to figures 20 and 21 it appears that they cause the increase of controlling moments in a permissible scope.

Verifying the operation of OSTS in the mode of searching the air space by the seekers of two rocket missiles simultaneously, with the consideration of forces coming from a sea ship with the condition of sea of 4 B

Figures 23–28 shows the forces coming from the movements of a ship floating on waves having an impact on the missile launcher mounted on its deck. Figures 31 and 32 show the trajectories of programmed movement of the seeker axis No. 1 and No. 2 respectively, and the trajectories of movement of rocket missiles axes, caused by the oscillations of a ship. The seeker of the first missile scans the air space on the surface of a single circular cone, while the seeker of the second missile is programmed in such a way so that after scanning the space on the surface of the first cone it started an additional search on the surface of the second circular cone.

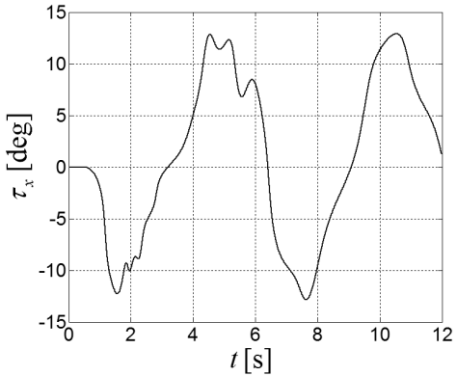

Fig. 23. Roll motion of the ship

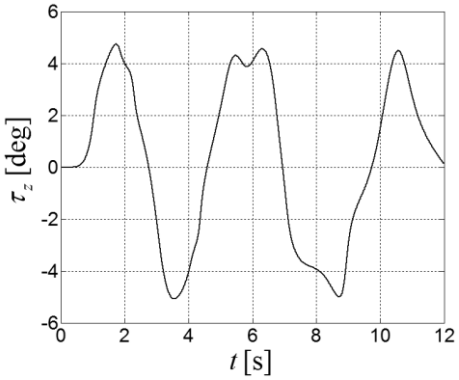

Fig. 24. Yaw motion of the ship

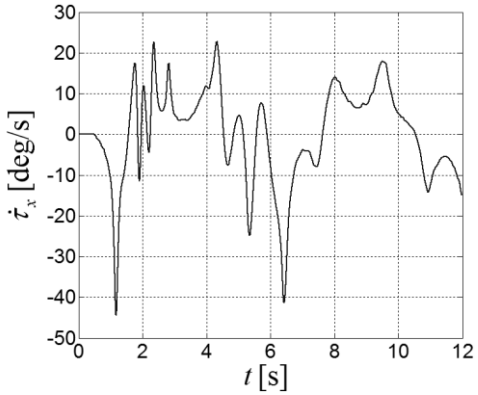

Fig. 25. Angular velocity roll motion

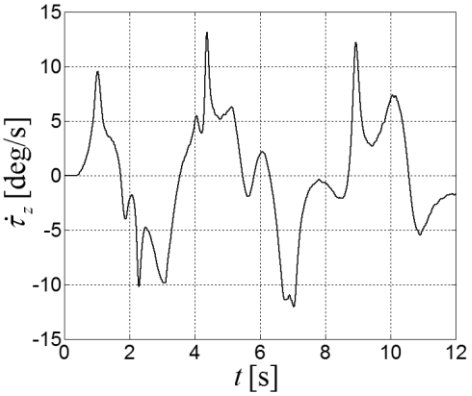

Fig. 26. Angular velocity yaw motion

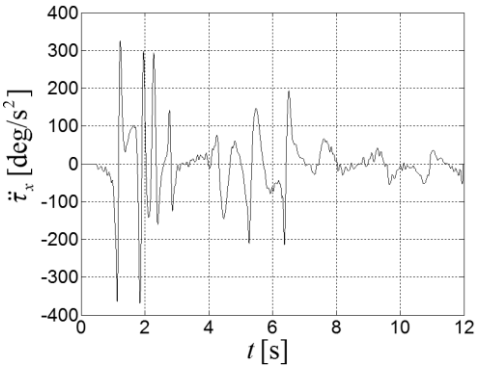

Fig. 27. Angular acceleration roll motion

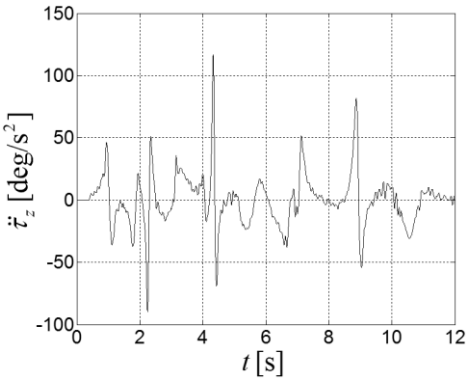

Fig. 28. Angular acceleration roll motion

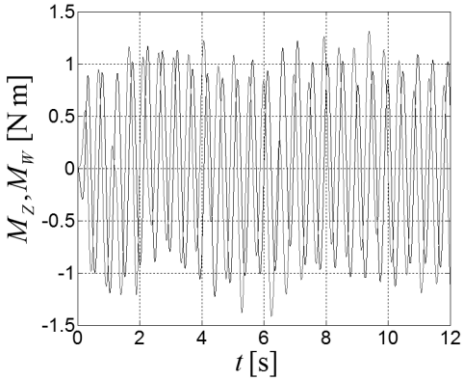

Fig. 29. Control moments of the first scanning seeker during the execution of movements from fig. 33

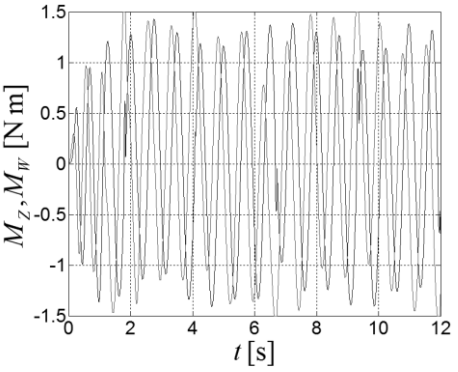

Fig. 30. Control moments of the second scanning seeker during the execution of movements from fig. 34

It appears from the diagrams of trajectories of movement performed by OSTS axis and missile axis shown in fig. 31 that the considered forces coming from the ship have a slight impact on the process of searching the air space by OSTS on the surface of a single circular cone, while it appears from figure 32 that the seeker will not manage to search the air space on the surface of the second circular cone. Having compared figures 29 and 30, it can be stated that the fact that the trajectories T_R shown in figure 31 do not overlap is caused by reaching maximum values $M_{\max}$ by controlling moments.

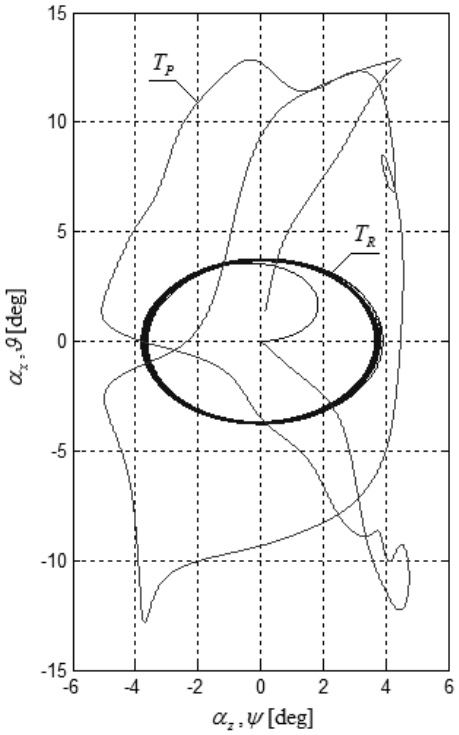

Fig. 31. Trajectory of the set T_Z and actual T_R movement of the first seeker axis and trajectory movement of the missile axis T_P, taking into account the movements of the ship

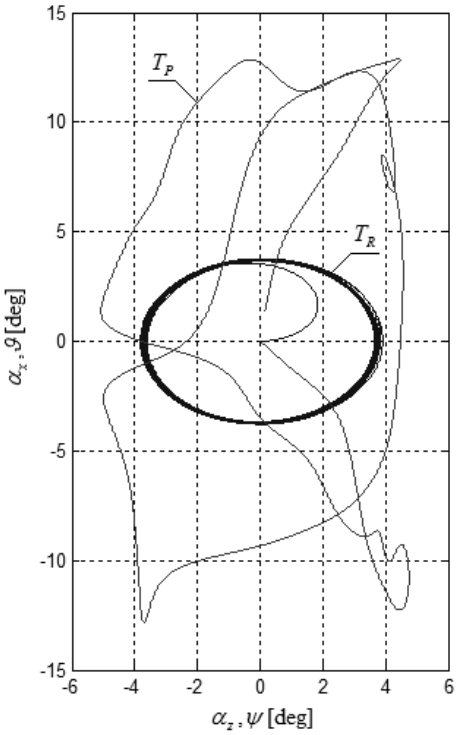

Fig. 32. Trajectory of the set T_Z and actual T_R movement of the first seeker axis and trajectory movement of the missile axis T_P, taking into account the movements of the ship

Verifying the impact of forces coming from the ship on the accuracy of determining the location of the target tracked by OSTS with the condition of sea of 3 B

In order to conduct the analysis of possibility of detecting and tracking an air target by the designed seeker with the simultaneous forces coming from the movements of the ship on waves, the disruptions working on OSTS presented in point 3.2 were considered. The simulation shown in figure 33 was conducted for flight speeds of targets: $v_{C1} = 380\,\text{m/s}$ and $v_{C2} = 360\,\text{m/s}$. The targets were located at the distance of 2500 m from the ship. Scanning the air space was done by two scanning and tracking seeker simultaneously. The process of selection of air targets by individual OSTS has been described in paper [7].

The coordinates of air targets in relation to OSTS axis at the moment of their detection amounted to respectively:

– for the target detected by OSTS 1: $\beta_x(t) = 0{,}884^{\circ}$, $\beta_z(t) = 0{,}473^{\circ}$;

– for the target detected by OSTS 2: $\beta_x(t) = -0{,}472^{\circ}$, $\beta_z(t) = 0{,}532^{\circ}$.

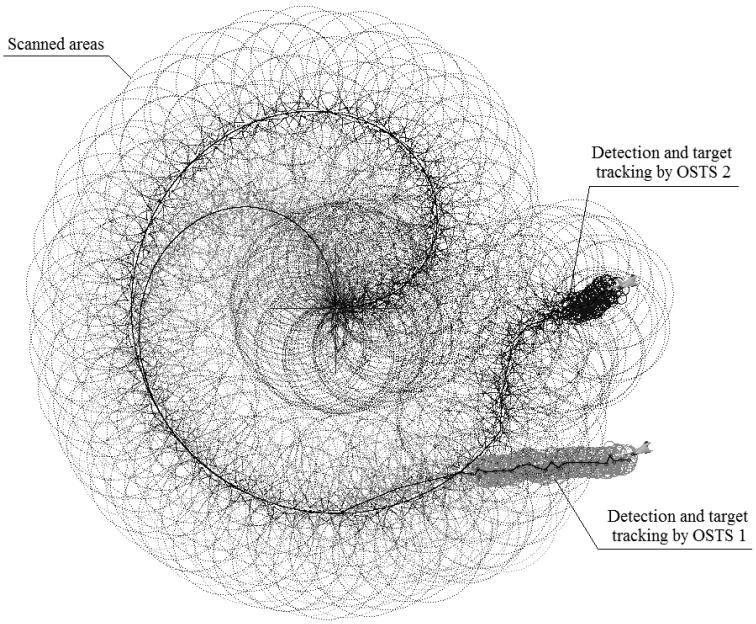

Fig. 33. The searching, detection and tracking of the target, taking into account the movements of the ship (minesweeper 207 M) — sea state 3 in Beaufort scale

It appears from the simulation shown in figure 33 that the disruptions coming from the oscillations of a sea ship type 'minesweeper type 207 M' with the condition of sea of 3 on the Beaufort scale do not have a negative impact on the process of detecting and tracking air targets by presented OSTS.

RESEARCH RESULTS AND CONCLUSIONS

The conducted analysis of impact of disruptions coming from the ship floating on waves (without the linear velocity) proves that the designed optical scanning and tracking seeker will be searching and tracking the detected air targets from the deck of a ship of small buoyancy amounting to 200 t (e.g. minesweeper type 207 M) with the condition of sea of 3 on the Beaufort scale effectively.

REFERENCES

[1] Begovic E., Day A. H., Incecik A., *Experimental Ship Motion and Load Measurements in Seeker and Beam Seas*, Atilla 2011, [in:] 9th Symposium in High Speed Marine Vehicles, 2011.05.26–2011.05.27, Naples, ID code: 44031.

[2] Das S. N., Das S. K., *Determination of Coupled Sway, Roll, and Yaw Motions of a Floating Body in Regular Waves*, 'Mathematical Problems in Engineering — Specjal Issue on Modeling Experimental Nonlinear Dynamics and Chaotic Scenarios', IJMMS 2004, 41, pp. 2181–2197.

[3] Gapiński D., *Analiza układu optoelektronicznego zmodyfikowanego koordynatora celu*, XIV Konferencja Automatyzacji i Eksploatacji Systemów Sterowania i Łączności ASMOR, Jastrzębia Góra, 9–11 października 2013, pp. 79–87 [*The analysis of an optoelectronic set of a modified target coordinator* — available in Polish].

[4] Gapiński D., Koruba Z., Krzysztofik I., *The model of dynamics and control of modified optical scanning seeker in anti-aircraft rocket missile*, 'Mechanical System and Signal Processing', 2014, Vol. 45, Issue 2, pp. 433–447.

[5] Gapiński D., Krzysztofik I., Koruba Z., *Analysis of the dynamics and control of the modified optical target seeker used in anti-aircraft rocket missile*s, 'Journal of Theoretical and Applied Mechanics', 2014, Vol. 52, No. 3, pp. 629–639.

[6] Gapiński D., Krzysztofik I., Koruba Z., *Stabilność zaprojektowanego koordynatora skanującego w przeciwlotniczym pocisku rakietowym*, 'Problemy Mechatroniki. Uzbrojenie. Lotnictwo. Inżynieria bezpieczeństwa, 2015, Vol. 6, No. 1, pp. 56–70 [*Stability of a designed scanning coordinator in an anti-aircraft missile* — available in Polish].

[7] Gapiński D., Krzysztofik I., *Programowa selekcja celów powietrznych wykrytych przez głowicę skanująco-śledzącą* [*Software based selection of air targets detected by a scan-track warhead*], [bilingual], 'Zeszyty Naukowe Akademii Marynarki Wojennej', 2014, No. 3, pp. 39–50.

[8] Gapiński D., *Optyczny koordynator skanujący*, patent PL 199721 B1, Urząd Patentowy Rzeczypospolitej Polskiej, 2008 [*Optical scanning coordinator* —available in Polish].

[9] Gapiński D., Stefański K., *A control of modified optical scanning and tracking seeker to detection and tracking air targets*, 'Solid State Phenomena', 2014, Vol. 2010, pp. 145–155.

[10] Gapiński D., Stefański K., *Control of designed target seeker, used in self-guided anti-aircraft missiles, by employing motors with a constant torque*, 'Aviation', 2014, Vol. 18, pp 20–27.

[11] Gapiński D., *Wpływ zmiany ustawień zwierciadeł skanujących zaprojektowanej głowicy skanująco-śledzącej na dokładność wyznaczania położenia celu*, 'Mechanika w Lotnictwie', 2014, Vol. II, pp. 393–400 [*The effect of changes in settings of scanning mirrors in a scan-track warhead on the accuracy of target position location* — available in Polish].

[12] Hu Q., Cai F., Yang C., Shi C., *An Algorithm for Interpolating Ship Motion Vectors*, 'TransNav the international Journal on Marine Navigation and Safety of Sea Transportation', 2014, Vol. 8, No. 1, DOI: 10.12716/1001.08.01.04.

[13] Ibrahim R. A, Grace M. I., *Modeling of Ship Roll Dynamics and Its Coupling with Have and Pitch*, 'Mathematical Problems in Engineering', Vol. 2010, DOI: 10.1155/2010/934714.

[14] Janowski W., *Matematyka — podręcznik dla wydziałów mechanicznych i elektrycznych politechnik*, Państwowe Wydawnictwo Naukowe, t. 1, wyd. VII, Warszawa 1973 [*Mathematics — a manual for mechanical and electric engineering departments of universities of technology* — available in Polish].

[15] Kornev N., *Ship Dynamics in waves*, Universität Rostock Fakultät für Maschinenbau und Schiffstechnik, Rostock 2011.

[16] Koruba Z., *Dynamika i sterowanie giroskopem na pokładzie obiektu latającego*, 'Monografie. Studia. Rozprawy', No. 25, Wyd. Politechniki Świętokrzyskiej, Kielce 2001 [*Dynamics and control of a gyroscope aboard a flying platform* — available in Polish].

[17] Koruba Z., *Elementy teorii i zastosowań giroskopu sterowanego,* 'Monografie, Studia, Rozprawy', M 7, Wyd. Politechniki Świętokrzyskiej, Kielce 2008 [*Elements of theory and application of a control moment gyroscope* — available in Polish].

[18] Koruba Z., Krzysztofik I., Dziopa Z., *An analysis of the gyroscope dynamics of an anti-aircraft missile launched from a mobile platform*, 'Bulletin of the Polish Academy of Sciences — Technical Sciences', 2010, Vol. 58, No. 4, pp. 651–656.

[19] Koruba Z., Osiecki J. W., *Budowa, dynamika i nawigacja pocisków rakietowych bliskiego zasięgu*, cz. 1, Wyd. Politechniki Świętokrzyskiej, Kielce 1999 [*Construction, Dynamics and navigation of shot-range missiles* — available in Polish].

[20] Koskinen K., *Numerical simulation of ship motion due to waves and manoeuvring*, Degree project in Naval Architecture second cycle, KTH Engineering Sciences, Stockholm 2012.

[21] Krzysztofik I., Osiecki J. W., *Wykrywanie i śledzenie celów*, Wyd. Politechniki Świętokrzyskiej, Kielce 2008 [*Detecting and tracking target*s — available in Polish].

[22] Maki A., Umeda N., *Bifurcation and Chaos in Yaw Motion of a Ship at Lower Speed in Waves and Its Prevention Using Optimal Control,* Proceedings of the 10th International Conference on Stability of Ships and Ocean Vehicles, 2009, pp. 429–440.

[23] Milewski S., Kobierski J. W., Chmieliński M., *Trenażery morskich zestawów rakietowo--artyleryjskich,* 'Zeszyty Naukowe Akademii Marynarki Wojennej', 2012, No. 3, pp. 87–100 [*Training simulators based on naval artillery and missile sets* — available in Polish].

[24] Milewski S., Kobierski J. W., *Szkolenie funkcyjnych okrętowych systemów rozpoznawczo--ogniowych z wykorzystaniem trenażera TR ZU-23-2MR*, 'Mechanika w Lotnictwie', Vol. I, pp. 241–254 [*Training operators of shipboard reconnaissance and fire conduct systems using TR ZU-23-2MR training simulator* — available in Polish].

[25] Pawlędzio A., *Badania modelowe kołysań swobodnych okrętu na wodzie spokojnej*, 'Zeszyty Naukowe Akademii Marynarki Wojennej', 2009, No. 3, pp. 29–38 [*Model-based study on ship free rotational motion on calm water* — available in Polish].

[26] Pawlędzio A., *Wyznaczanie kąta przechyłu dynamicznego okrętu na podstawie badań modelowych*, 'Zeszyty Naukowe Akademii Marynarki Wojennej', 2009, No. 2, pp. 29–38 [*Calculating the ship angle of dynamic heel using model based investigations* — available in Polish].

[27] Resnick R., Halliday D., *Fizyka 1*, Wyd. Naukowe PWN, Warszawa 1997 [*Physics 1* — available in Polish].

[28] Spyrou K. J., *The Nonlinear Dynamics of Ships in Broaching*, 'Marie Curie Fellowships Annals', 2000, Vol. 1.

[29] Wełnicki W., *Mechanika ruchu okrętu*, Wyd. Politechniki Gdańskiej, Gdańsk 1989 [*Ship motion mechanics* — available in Polish].

ANALIZA WPŁYWU ZAKŁÓCEŃ POCHODZĄCYCH OD OKRĘTU NA DOKŁADNOŚĆ WYZNACZANIA POŁOŻENIA ŚLEDZONEGO CELU POWIETRZNEGO PRZEZ ZMODYFIKOWANĄ OPTOELEKTRONICZNĄ GŁOWICĘ SKANUJĄCO-ŚLEDZĄCĄ

STRESZCZENIE

W artykule przedstawione zostały wyniki badań mających na celu określenie wpływu zakłóceń pochodzących od ruchu okrętu na dokładność wyznaczania położenia śledzonego celu przez zmodyfikowaną optoelektroniczną głowicę skanująco-śledzącą (OGSS). Podstawowym zadaniem OGSS jest wykrycie, a następnie precyzyjne śledzenie wykrytego celu powietrznego emitującego promieniowanie w zakresie podczerwieni.

Słowa kluczowe:
mechatronika, głowica samonaprowadzająca, wykrywanie, śledzenie, zakłócenia.